RESOLVING THE FAN-SPINE STRUCTURE OF A SMALL-SCALE CHROMOSPHERIC JET WITH THE NEW SOLAR TELESCOPE

Zhicheng Zeng[1,2], Bin Chen[1,3], Wenda Cao[1,2] and Philip R. Goode[2]

1.Center for Solar-Terrestrial Research, New Jersey Institute of Technology, 323 Martin Luther King Blvd., Newark, NJ 07102, USA

2. Big Bear Solar Observatory, 40386 North Shore Lane, Big Bear City, CA 92314, USA

3. Harvard-Smithsonian Center for Astrophysics, 60 Garden Street, Cambridge, MA 02138, USA

ABSTRACT

Jets present ubiquitously in both quiet and active regions of the Sun. It is widely believed that they are driven by magnetic reconnection. A fan-spine structure has been frequently reported in some coronal jets and flares, which is considered to be a signature of ongoing magnetic reconnection in a topology consisting of a magnetic null connected by a fan-like separatrix surface and a spine line. However, for small-scale chromospheric jets, clear evidence of such structures is rather rare, although they are implied in earlier works that show an inverted-Y-shaped feature. Here we report high-resolution (0″.16) observations of a small-scale chromospheric jet observed by the New Solar Telescope (NST) using 10830 Å filtergrams. Of particular interest is that bi-directional flows were observed across the separatrix regions in 10830 Å images, suggesting that the jet was produced due to reconnection. Most features predicted in a fan-spine structure were clearly resolved by the NST, including the spine and the fan-like surface, as well as the loops before and after the reconnection. A major part of this fan-spine structure, with the exception of its bright footpoints and part of the base arc, was invisible in the extreme ultraviolet and soft X-ray images, indicating that the reconnection occurred in the upper chromosphere. Our observations suggest that the evolution of this chromospheric jet is consistent with a two-stage reconnection scenario proposed by Török et al. (2009).

Subject headings: Sun: chromosphere — Sun: corona — Sun: activity

1. INTRODUCTION

Jets are the phenomena of collimated plasma ejecta shooting out from a localized region in the low solar atmosphere. They have been observed in optical, (extreme) ultraviolet

(UV/EUV), and X-ray wavelengths with various sizes, speeds, and durations (Canfield 1996; Savcheva et al. 2007; Jiang et al. 2007; Liu et al. 2009; Nishizuka et al. 2011; Tian et al. 2014). Jets usually show a strong tendency to recur, suggesting their association with a prolonged process of magnetic flux emergence and cancellation at their bases (Kurokawa & Kawai 1993; Liu & Kurokawa 2004). Observations at various wavelengths (Shibata et al. 1992; Canfield 1996; Shimojo et al. 1998; Liu et al. 2009) and MHD simulations (Archontis et al. 2005; Nishizuka et al. 2008; Pariat et al. 2009) support a scenario in which a jet is driven by magnetic reconnection between newly emerging magnetic fluxes and overlying ambient magnetic fields of opposite polarity. This process could result in a configuration for magnetic reconnection at a three-dimensional (3D) magnetic null point, connected by a fan-like separatrix surface and a spine line along which the reconnected field lines approach or recede from the null (Lau & Finn 1990; Antiochos 1998, see, e.g., the schematic in Fig. 1 of Liu et al. 2011 and Fig. 5d of this paper). Signatures of such a "fan-spine" topology have been reported in various contexts that involve magnetic reconnection, which include X-ray jets (Shibata et al. 1994; Shimojo et al. 1996), anemone-like active regions (Asai et al. 2008), and "circular-ribbon" flares (Masson et al. 2009; Sun et al. 2013; Wang & Liu 2012; Liu et al. 2015).

For small-scale chromospheric jets, however, direct observations of fan-spine structures are rather rare, although the existence of a fan-spine structure is strongly implied by the frequently observed inverted-Y-shaped structure of the jet base (Shibata et al. 2007; Nishizuka et al. 2008). The best evidence heretofore was reported by Liu et al. (2011): they used Hinode/SOT Ca II H observations to track cool ($\lesssim$20,000 K), coronal-rain-like flows draining down to the photosphere following a jet, which resembled a dome-like shape at the jet base. Yet the inner spine under the dome (c.f., Fig 5d) was not seen. As the authors suggested, this is probably because that the Ca II H band was not sensitive to the temperature of the inner spine material.

He I imaging at 10830 Å has been proven to be an excellent method for observing plasma with temperatures characteristic of the upper chromosphere and transition region (>20,000 K). This is because the He I line requires a high collisional excitation level and/or a sufficiently high EUV radiation field. One mechanism is photo-ionization followed by recombination, or the "PR" mechanism (Zirin 1975), in which neutral helium can be ionized by high-energy photons (shortward of 504 Å) and then recombine to the excited $n = 2, 3$ levels of orthohelium. Another appeals to the rapid collisional mechanism (CM) in which atoms are excited, before they have a chance to be ionized, by electrons with temperatures higher than those expected in the ionization equilibrium (Jordan 1975; Andretta et al. 2000; Pietarila & Judge 2004).

Here we exploit high-resolution (0″.16) He I 10830 Å imaging utilizing the New Solar Telescope (NST) to resolve the fan-spine structure in a small-scale chromospheric jet. The instruments and data reduction are discussed in Section 2. Section 3 presents observational

also a signature of an ongoing magnetic reconnection.

4. DISCUSSION AND CONCLUSIONS

We present high-resolution NST observations of a small-scale recurrent jet event using the He I 10830 Å filter, which is sensitive to upper chromospheric temperatures. The NST observations are complemented by EUV and X-ray data from SDO/AIA, Hinode/XRT, and RHESSI that cover a broad temperature range from ~1 MK to >10 MK.

The NST He I images reveal detailed structures of the recurrent jet. In particular, the jet consists of an elongated spine along the direction of ejection and a fan-shaped arc at the base of the jet, closely matching the fan-spine reconnection geometry for jet production. The fan-shaped arc at the base of the jet is only 10″ wide, spanning over the penumbral region of a spot with a dominating positive magnetic polarity. According to the reconnection picture, the inner spine of the jet that connects to the magnetic null point (seen in He I in absorption) should be rooted in a newly emerged magnetic flux with negative polarity. It is difficult, though, to confirm this using the HMI line-of-sight magnetogram directly, because the negative polarity region was presumably very small and the event occurred very close to the limb. However, there are multiple lines of evidence supporting the fan-spine reconnection scenario: First, the root of the inner spine (seen in He I in absorption) coincides with localized Hα, EUV, and X-ray emissions at the same location (c.f., Fig. 3, indicated by the blue arrow). This suggests intensive heating at the root of the inner spine (by either precipitated particles or thermal conduction) resulted from magnetic reconnection at the magnetic null point. Second, bi-directional plasma flows are observed at the onset of both stages of the jet. They originate from a common location at the base of the jet and near the apex of the fan structure, which is probably the site of the magnetic null point where reconnection occurs. We note that these bi-directional plasma flows could not be reconnection outflows themselves, as their speeds (~20-30 km/s) are much lower than the local Alfvén speed (~ 200 km/s for 10 G and density of 10^{10} cm^{-3}). Instead, they could be secondary pressure-driven flows expelled from the reconnection site.

We conclude that the observed features in the two major stages of the jet evolution are similar to the two-stage magnetic reconnection scenario of jets proposed by Török et al. (2009), as depicted in the two schematic cartoons in Fig. 5.

The first stage starts when reconnection occurs between the emerged negative magnetic flux and the ambient, unipolar field (Fig. 5c). Reconnected loops shrink downward to the left side of the null point and are heated by the released energy (~~in~~ pink ~~color~~). These heated loops appear as a bright patch in the AIA EUV images near the footpoint, but are resolved in the He I images as a bundle of bright loops on the left side (Fig. 5a). The energy released from reconnection also drives heated plasma from the null point upward along the spine field

results of the jet using the NST and other instruments in EUV and X-rays. In Section 4, we consider implications and interpretation of these data.

2. OBSERVATION AND DATA REDUCTION

On July 8, 2012, we used the 1.6 meter aperture NST at the Big Bear Solar Observatory (NST/BBSO; Goode & Cao 2012; Cao et al. 2010b) to observe NOAA active region (AR) 11515, which located close to the west solar limb. NST's off-axis design eliminates any central obscuration, which vastly reduces stray light. High spatial resolution images were obtained by using a broad band filter (bandpass: 10 Å) containing the well-known TiO lines, as well as a narrow band filter (bandpass: 0.5 Å) placed in the blue wing of the He I 10830 Å multiplet. Images in Hα line center and blue wing (-0.8 Å) were also acquired for comparison.

The 10830 Å Lyot filter was made by the Nanjing Institute for Astronomical and Optical Technology. This narrow-band filter was tuned to -0.25 Å relative to the two blended strongest components of the multiplet (at 10830.3 Å), making the filtergram capable of imaging fine details of the chromospheric material and meanwhile, capturing the underlying photospheric features, which are very helpful for co-aligning with other instruments. A high sensitivity HgCdTe CMOS IR focal plane array camera (Cao et al. 2010a) was employed to acquire the 10830 Å data at a cadence of 10 s. With the aid of high order adaptive optics and speckle reconstruction based post-processing method (the KISIP code; Wöger & von der Lühe 2007; Cao et al. 2010c), diffraction limited resolution ($\frac{\lambda}{D}$) images in the three bands were achieved (the angular resolution is $\sim 0\farcs16$ for 10830 Å).

The Atmosphere Imaging Assembly (AIA; Lemen et al. 2012) on board the *Solar Dynamic Observatory* (*SDO*; Pesnell et al. 2012) provides continuous coverage of the Sun at multiple UV and EUV passbands, with a cadence of 12 s and spatial resolution of $1\farcs5$ arcsecs. The AIA data were used to investigate plasma associated with the jet at coronal temperatures from 1 to 10 MK. This event was observed by the X-Ray Telescope (XRT; Golub et al. 2007) on board Hinode (Kosugi et al. 2007), which extends the temperature coverage to > 10 MK. The *Reuven Ramaty High Energy Solar Spectroscopic Imager* (*RHESSI*; Lin et al. 2002) and the Gamma-ray Burst Monitor (GBM; Meegan et al. 2009) aboard the *Fermi* Gamma-ray Space Telescope also observed this event in hard X-rays (HXRs). RHESSI images are reconstructed using the PIXON algorithm (Hurford et al. 2002) based measurements from detectors 3, 5, 6, 7 and 8.

White-light continuum images from the Helioseismic and Magnetic Imager (HMI; Scherrer et al. 2012) on board SDO were used as the intermediary for co-aligning the AIA and NST images. AIA and HMI images were co-aligned with each other using telescope pointing information in the image FITS headers. The NST TiO and 10830 Å images were co-aligned using common features seen by both filtergrams, such as sunspots and granules (visible in

the field-of-view despite limb darkening). The accuracy of the co-alignment is expected to be better than 0.″6.

3. RESULTS

The jet event under study occurred repeatedly around the east edge of the leading sunspot in AR 11515 from 18:19 UT to 18:50 UT. Fig. 1 shows images of the jet at ~18:39 UT in 10830 Å (panels a and x), TiO (panel y), Hα(panel z), EUV (panel b), and soft X-ray (SXR; panel c). The jet was located near the footpoint of a closed coronal loop system as shown in the XRT Al-thick image (Fig. 1b and c). The second row of Fig. 1 shows a closer view of the base of the jet (green box in Fig. 1a), rotated by 110° counterclockwise to an upright orientation. The base of the jet appears as a fan-like structure in the 10830 Å filtergram (Fig. 1x). This structure can also be distinguished in the Hα blue wing images, which are, however, badly saturated thus not shown here. Meanwhile, this structure is totally absent from all AIA EUV images, indicating that its temperature is well below coronal values. The footpoints of the fan-like loops in 10830 Å coincides very well with footpoint brightenings in AIA 171 Å images (yellow contours in Fig. 1x), suggesting strong heating in the footpoint area. The size of the fan is ~10″, spanning over the penumbral regions of a spot with positive magnetic polarity (Fig. 1y). A dark strand is seen in the 10830 Å image extending from the apex of the fan-like structure downward to the photosphere (indicated by a red arrow in Fig. 1x). Its root coincides with a brightening in the Hα line center image (Fig. 1z).

The evolution of the jet can be generally divided into two major stages as delineated in the space-time plot of the AIA 304 Å intensity (Fig. 1d). The space-time plot is obtained at a slice positioned along the jet (dashed line in Fig.1a). The onset of each stage is characterized by a strong footpoint emission in AIA 304 Å (18:18:50 UT and 18:38:40 UT for the first and second stage, respectively). The AIA 304 Å footpoint brightenings in the two stages correlate well with impulsive peaks in the 1–8 Å soft X-ray (SXR) derivative (from GOES, the Geostationary Operational Environmental Satellite) and the 12–25 keV HXR count rate from Fermi/GBM. This correlation suggests that the jet evolution is strongly correlated with electron acceleration and/or strong plasma heating processes (Kane et al. 1979; Fletcher & Hudson 2001).

Fig. 2 shows the evolution of the jet in the first stage observed in He I 10830 Å, AIA 304 Å and Hα line center (an animation is available online for this process: stageI.mpg). The jet is visible in 10830 Å as a dark outgoing ejecta, which appears bright in AIA 304 Å and Hα. With NST's unprecedentedly high resolution, a fan-like structure is clearly seen at the base of the jet in the 10830 Å images, consisting of multiple individual loops. The loop system on the left side of the jet is brighter than that on the right, which appears as an unresolved brightening in the AIA 304 Å images (blue arrows in Fig. 2). The evolution of the fan-like loops suggests that magnetic reconnection is likely occurring between the loop

systems on both sides of the jet. To visualize this, we select a curved slice along the fan structure (dashed line in Fig. 2b) and obtain the 10830 Å intensity on this slice as a function of time, i.e., a space-time plot (Fig. 4a) in the space-time plot. At ~18:21:10 UT, two tracks with opposite slopes (directed by red arrows) appear at the slit location of 8″ (indicated by a white arrow in Fig. 4a). These two tracks correspond to bi-directional plasma outflows (at 30 km s^{-1}) emanating from a common region. In the 10830 Å image, this region is located between the left and right loop systems near the apex of the fan-like structure (marked by an "x" symbol in Fig. 2b), presumably the site of magnetic reconnection. The time when the bi-directional outflows occur coincides very well with the footpoint brightening seen in AIA 304 Å (c.f., Fig. 1d).

The second stage starts from 18:39 UT, ~10 minutes after the first stage (an animation is available online: stageII.mpg). In contrast to the first stage, the AIA 304 Å intensity at the jet base is dominated by the emission at the right side of the jet (Fig. 3d-f). In 10830 Å images, the AIA brightening near the footpoint is resolved as a bundle of small-scale loops. The fan-like surface is clearly visible at the jet base, composed with alternately black and white fibrils with thickness of ~0.3″ (Fig. 3a). After 18:41 UT, a dark spine near the center of the jet becomes evident in 10830 Å, Hα, and AIA EUV (indicated by white arrows in Fig. 3). This dark spine extends further downward across the fan structure and rooted at the photosphere, representing as the "inner spine" in the fan-spine reconnection geometry (c.f., Fig 5d). The foot of the inner spine is co-spatial with a Hα brightening (indicated by a blue arrow in Fig. 3g) and a footpoint X-ray source (observed by RHESSI at 10-18 kev, green contours in Fig. 3d). During the late phase of stage 2, bright and small-scale loops form at the right side of the jet spine in 10830 Å (Fig. 3c), whereas a curtain-like surge (5″ across) extends to at the left side, which appears dark in 10830 Å and bright in EUV 304 and Hα.

In order to track the evolution of the jet and the associated loop reconfiguration in the second stage, we select two slices in the 10830 Å and AIA 171 Å image series and obtain the corresponding space-time plots: one slice is placed along the jet spine, and another is drawn across the spine (slices 2 and 3 in Fig. 3c, respectively). The results are shown in Fig. 4b and c, respectively. The recurrent jet in this stage shows two jet episodes, one starts at 18:38:40 UT and another at ~18:42:00 UT. The measured speed of the jet is as high as 120 kms^{-1}. Interestingly, the jet is dominated by bright 10830 Å emission at low altitudes, and is gradually taken over by the EUV 171 emission as it propagates to higher altitudes (Fig. 4b). The running-ratio space-time plot in Fig. 4c (for slice 3) is used to identify flow patterns near the jet base. Similar to the case in the first stage, at the onset of this stage (~18:38:40 UT), bi-directional flows (at ~20 km/s) emanate from the slit location of 4″ (denoted by a white arrow in Fig. 4c), which is presumably the site of magnetic reconnection driving the jet (marked by an "x" symbol in Fig. 3c). During the second episode of the jet at 18:42:00 UT, the spine extends like a curtain in the He I filtergrams (animation stageII.mpg), when another flow appears in the space-time plot (denoted by a yellow arrow in Fig. 4c). This flow corresponds to the sliding motion of magnetic field lines toward the left side of the jet spine,

lines as the jet material seen as emissions in EUV, 10830 Å and Hα (Fig. 2 left column; depicted in Fig. 5c in shaded pink color). Simultaneously, cool plasma is also ejected at the right side of the jet spine due to the "slingshot effect", which is especially evident during the phase of decay (indicated by the red arrow in Fig. 2i; depicted in Fig. 5c in shaded gray area). It is consistent with previous studies, which argued that hot (EUV and X-ray) and cold (Hα) plasma ejections can exist side-by-side (Shibata et al. 1992; Canfield 1996; Chae et al. 1999).

The second stage corresponds to a fully-developed state of the fan-spine reconnection geometry, when the magnetic loops at the left side of the null point reconnect with the ambient fields on the right (Fig. 5d). During this stage, the reconnected loops are visible at both sides and form a complete fan-shaped structure (Fig. 5b), separated by an inner spine near the center. The dark and bright fibril-like loops consisting of the fan structure (seen in 10830 Å) represent a mixture of heated and cooled loops formed by the repeated reconnection process at the magnetic null point (Fig. 5b). The reconnection also produces accelerated particles and/or thermal conduction fronts, which propagate along the inner spine and result in strong footpoint X-ray emissions (blue patch in Fig. 5d, EUV, 10830 Å and Hα). Different from Stage I, the reconnection between the emerging flux on the left and the ambient field on the right may play a dominant role in this stage, resulting in relatively brighter reconnected loops on the right (pink field lines) and curtain-like surges toward the left side of the jet spine due to the slingshot effect (gray patch above the pink field line).

We attribute our clear detection of the fan-spine structure to not only NST's superb sub-arcsec angular resolution, but also the special emission conditions for the 10830 Å line. The fan is completely absent in all AIA and XRT bands but clearly visible in He I, suggesting that the fan should consist of plasma at upper chromospheric temperatures ($\leq$20000 K) to which AIA and XRT are not sensitive. The He I emission is interpreted to be from the radiation of helium atoms at a metastable level excited by thermal collisions (i.e., the CM mechanism). The PR mechanism of He I emission is unfavorable for our case since there is insufficient EUV emission in the fan.

In both stages, the outer spine is observed as a collimated jet consisting of both hot and cool material. This is likely associated with the ejection of both heated plasma from the reconnection site, as well as cool material due to the sling-shot effect of the reconnected field lines. The inner spine, on the other hand, represents field lines directly connected to the magnetic null point. Its dark appearance in all filters (10830 Å, Hα and EUV) suggests a density depletion at the inner spine location. This is possibly associated with strong heating at the null point combined with efficient thermal conduction along the inner spine field line. The strong heating scenario is supported by the existence of a >10 MK X-ray source at the footpoint of the inner spine. Although very unlikely, we could not, however, rule out the possibility of the dark inner spine being associated with a cool filament-like structure that is fortuitously aligned with the jet direction, causing an absorption feature at all bands.

To summarize, the sub-arcsecond resolution of the NST, combined with the unique sensitivity of the He I 10830 Å line to upper chromospheric plasma of certain temperatures, provide a clear view of a chromospheric jet with a fan-spine geometry. We emphasize that although numerous cases of chromopheric jets have been reported with an anemone or inverted Y-shape, our observations, for the first time, reveal every element of the fan-spine structure predicted in the theoretical jet model. The evolution of the jet observed in 10830 Å, Hα, EUV, and X-ray wavelengths is consistent with a two-step reconnection scenario for jet formation. Our results will motivate further studies on chromospheric jets using high-angular-resolution observations as well as more detailed modelling approaches.

We thank BBSO observing staff and instrument team for their support. We thank Dr. Haisheng Ji for providing the narrow-band 10830 Å Lyot Filter. SDO is a project of NASA. Z. Z. and W. C. acknowledge the support of the US NSF (AGS-xxx and AGS-xxx), NASA (xxx), and AFOSR (FA xxx and FA xxx). B. C. acknowledges the support by NSF (xxx) and NASA (xxx).

REFERENCES

Andretta, V., Jordan, S. D., Brosius, J. W., et al. 2000, The Astrophysical Journal, 535, 438

Antiochos, S. K. 1998, The Astrophysical Journal Letters, 502, L181

Archontis, V., Moreno-Insertis, F., Galsgaard, K., & Hood, A. W. 2005, The Astrophysical Journal, 635, 1299

Asai, A., Shibata, K., Hara, H., & Nitta, N. V. 2008, The Astrophysical Journal, 673, 1188

Canfield, R. C. 1996, The Astrophysical Journal, 464, 1016

Cao, W., Coulter, R., Gorceix, N., & Goode, P. R. 2010a, in Society of Photo-Optical Instrumentation Engineers (SPIE) Conference Series, Vol. 7742, Society of Photo-Optical Instrumentation Engineers (SPIE) Conference Series

Cao, W., Gorceix, N., Coulter, R., et al. 2010b, Astronomische Nachrichten, 331, 636

Cao, W., Gorceix, N., Coulter, R., et al. 2010c, in Society of Photo-Optical Instrumentation Engineers (SPIE) Conference Series, Vol. 7735, Society of Photo-Optical Instrumentation Engineers (SPIE) Conference Series

Chae, J., Qiu, J., Wang, H., & Goode, P. R. 1999, The Astrophysical Journal Letters, 513, L75

Fletcher, L., & Hudson, H. 2001, Solar Physics, 204, 69

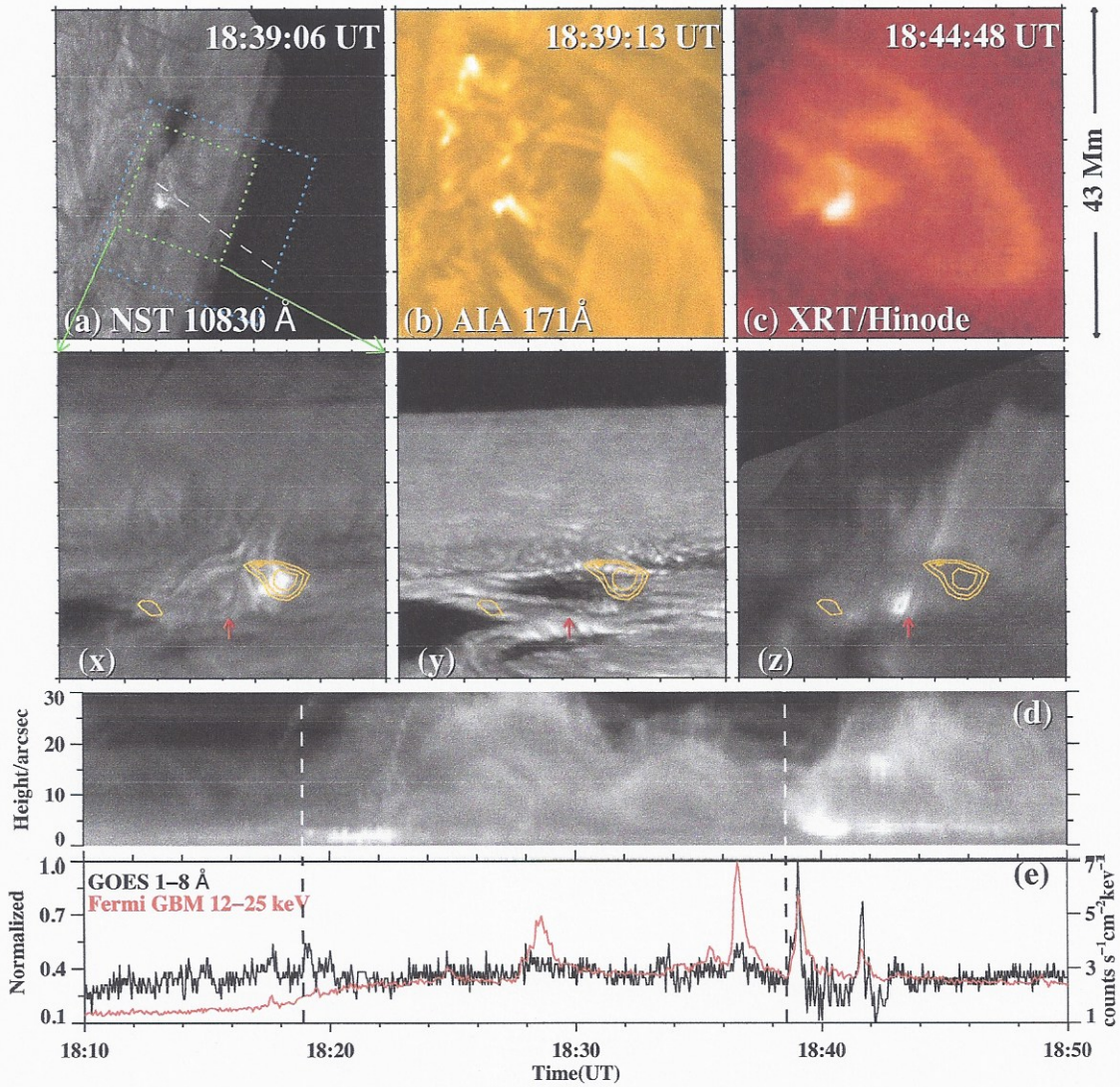

Fig. 1.— Snapshot of the observations: (a) A sample 10830 Å filtergram observed with the NST/BBSO. The blue boxes encompass the field-of-view of the images in Fig. 2 and 3. (b) AIA 171 Å. (c) XRT/Hinode. Panel (a-c) have the same field-of-view of 43 Mm × 43 Mm. The green boxed area in panel a is enlarged and rotated in panels (x-z). (x) 10830 Å filtergram, which clearly shows the fan structure. (y) TiO image (18:39:13 UT). (z) Hα line center (18:39:27 UT). The contours are from AIA 171 Å. Red arrows points to the footpoint of a dark strand in 10830 Å. (d) Space-time plot made from AIA 304 Å images. Slit position is indicated by a white dashed line in (a). (e) Light curves of normalized GOES derivative flux (black) and Fermi X-ray (red). Vertical dashed lines in (d) and (e) denote the start time of each stage.

↳, as well as pointing toward the fan.

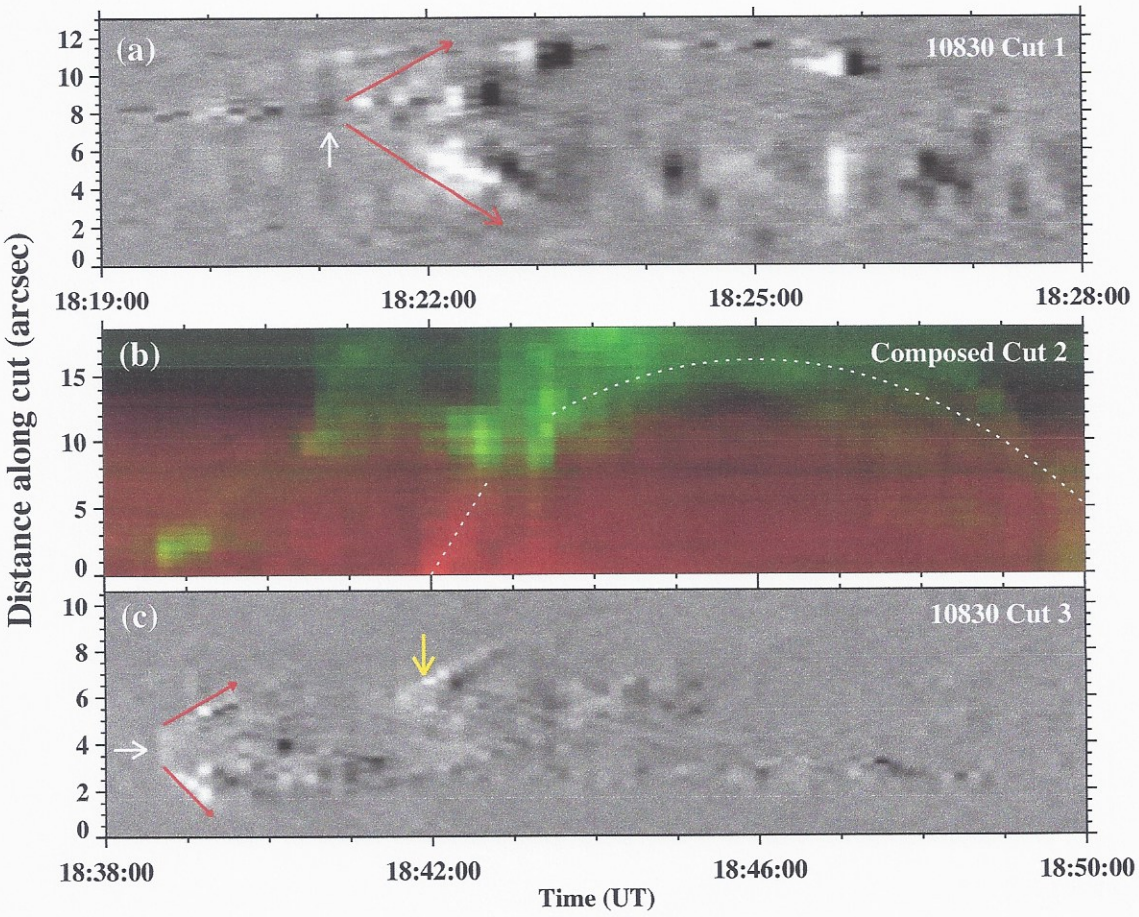

Fig. 4.— Space-time plots showing the evolution of the jet. (a) Space time plot of 10830 Å along Cut 1. The speed of the flows are ~30 km/s. (b) Composite space-time plots of AIA 171 Å (green) and 10830 Å (red) along Cut 2. Straight dotted line indicates the speed of the ejecta (~120 km/s) while the curved dotted line outlines the parabolic trajectory with the gravitational acceleration ~-273 m s^{-2}), respectively. The horizontal dashed line depict the height of the cross along the slit in Fig. 3. (c) Space-time plots of 10830 Å along Cut 3. The white arrows point to the start of the bi-directional plasma flows while the red arrows denotes the direction of the flows. The yellow arrow indicates the extension of the spine of the jet at 18:42:00 UT.

maybe one white arrow

to use two different colors to avoid confusion or dash-dot or ...

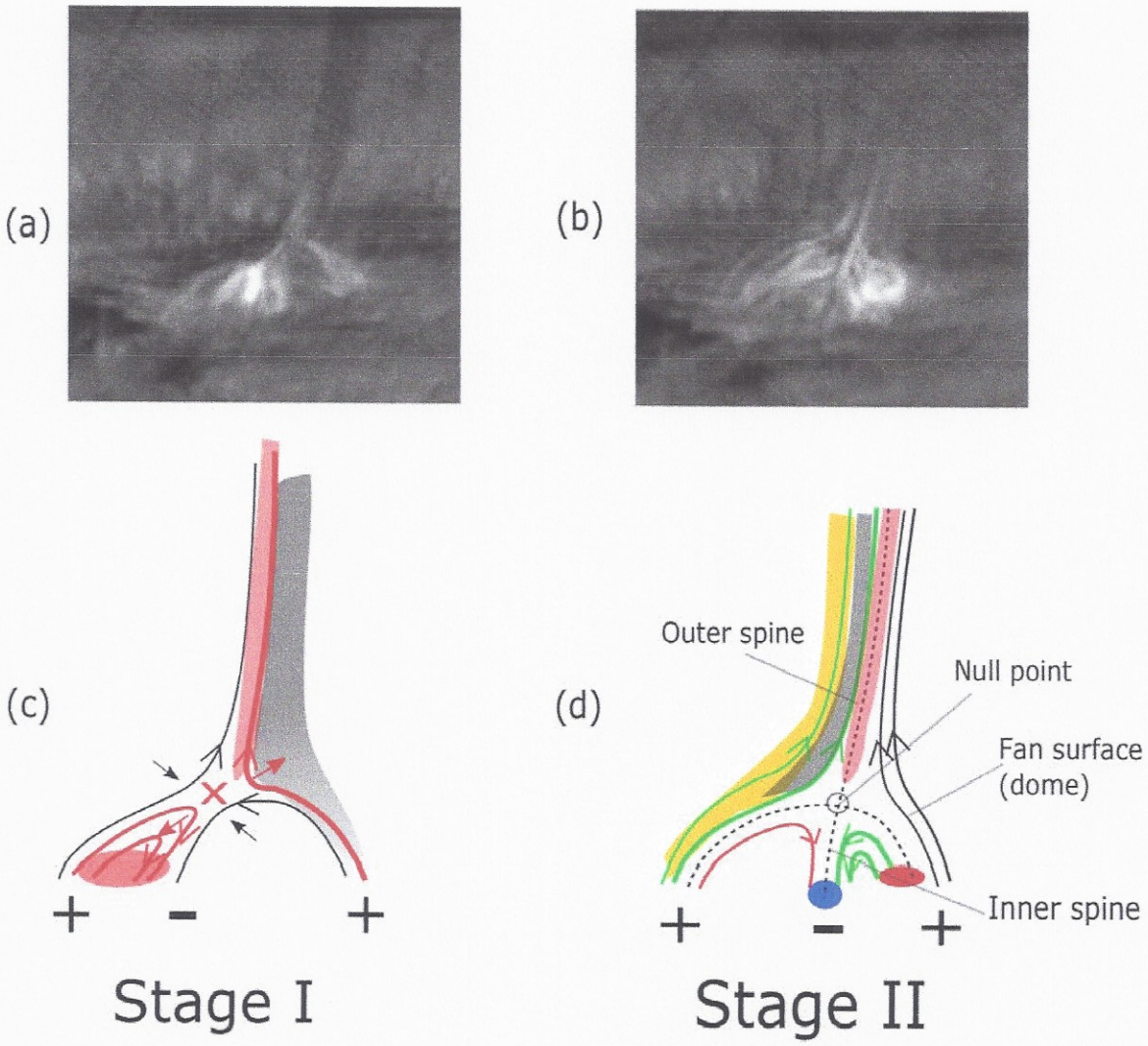

Fig. 5.— Panels a and b are selected images in 10830 Å with the prominent structure of the two stages. Panels c and d are schematic depiction of the jet ~~of~~ the two stages. Here red and green lines represent reconnected field lines in the first and second stage, respectively. Magnetic polarity is denoted by ±. The pink feature represent the emission as seen in AIA. In panel c, the dark features represent the surges in Hα and He I. Black and red arrows depict the connection sequence. In panel d, the yellow feature is surge in He I (emission) and AIA 304. Blue oval represents the RHESSI X-ray source. Dotted lines outline the separatrix layer.